Supporting Information

Highly improved performance in $Zr_{0.5}Hf_{0.5}O_2$ films inserted by graphene oxide quantum dots layer for resistive switching nonvolatile memory

Xiaobing Yan,[1,4*] Lei Zhang,[1] Yongqiang Yang,[2] Zhenyu Zhou,[1] Jianhui Zhao, [1] Yuanyuan Zhang,[1] Qi Liu,[3] Jingsheng Chen[4]

[1] *College of Electron and Information Engineering, Key Laboratory of Digital Medical Engineering of Hebei Province, Key Laboratory of Optoelectronic Information Materials of Hebei Province, Hebei University, Baoding 071002, P. R. China*

[2]*Jiangsu Province Special Equipment Safety Supervision and Inspection Institute · Branch of Wuxi, National Quality Supervision and Inspection Center of Graphene Products (Jiangsu), Wuxi2147174, P. R. China*

[3]*Key Laboratory of Microelectronic Devices & Integrated Technology, Institute of Microelectronics, Chinese Academy of Sciences, Beijing 100029, P. R. of China*

[4]*Department of Materials Science and Engineering, National University of Singapore, Singapore 117576, Singapore*

*Corresponding author: xiaobing_yan@126.com

Ⅰ The GOQDs specimens

We can observe that the solution of GOQDs is uniform as shown in Fig. S1, and it shows that GOQDs are evenly distributed inside the solution.

Figure S1. GOQDs solution specimens.

Ⅱ The XRD of the device.

As shown in Fig. S2, two peaks can be ascribed to Pt (111) and Si (100). Therefore, the $Zr_{0.5}Hf_{0.5}O_2$ films is amorphous through the analysis of the picture of XRD data. From the work of others, we know that amorphous materials can act as a function layer for resistive switching device.[1-3]

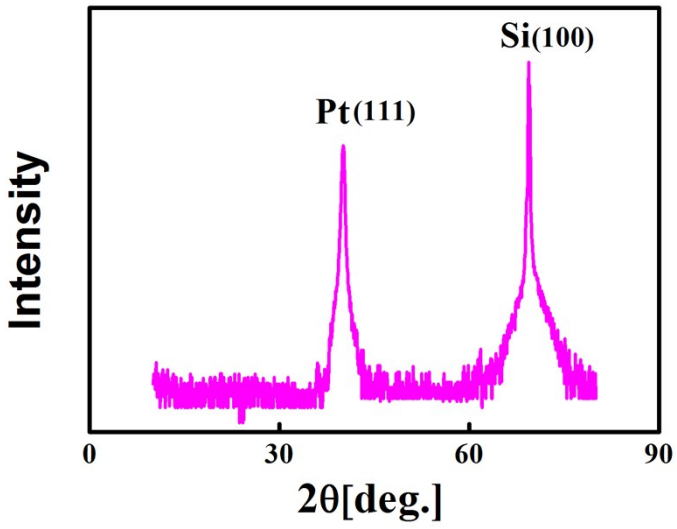

Figure S2. XRD of the device.

Ⅲ The I-V curves of 200 cycles for the two kinds of devices

In this work, we test I-V of the two kinds of devices with and get the following data as shown in Fig. S3. We can intuitively observe that the I-V circulation of the device with GOQDs is more concentrated than that of the device without GOQDs.

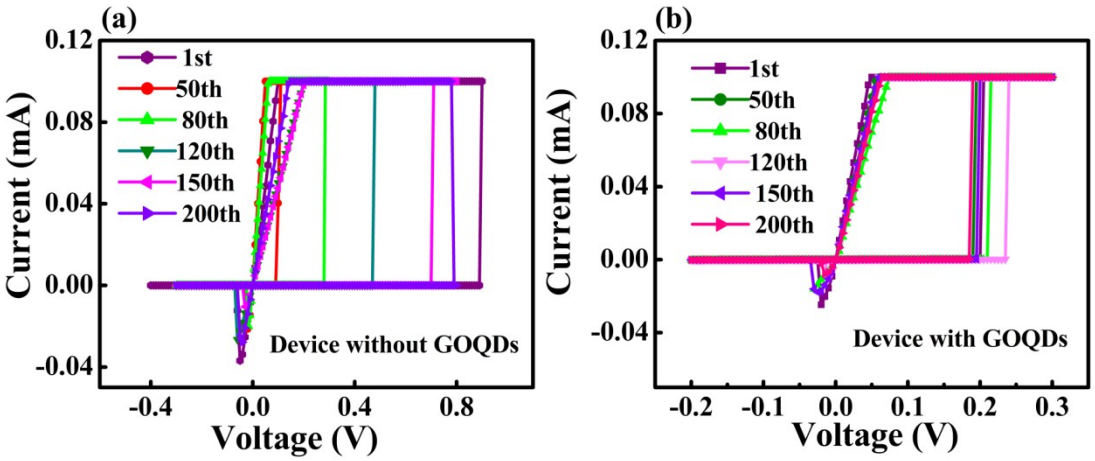

Figure S3. The I-V curves. (a) The I-V curves for 200 continuous RS cycles of the Ag/ZHO/Pt device, (b) The I-V curves for 200 continuous RS cycles of the Ag/ZHO/GOQDs/ZHO/Pt device.

Ⅳ The statistic distributions of LRS and HRS

The switching resistances at turn-on and turn-off states for 200 cycles' tests fluctuated in small ranges as described in Fig. S4(a). The statistic distributions of LRS and HRS were relative centralized as shown in Fig. S4(b). The HRS resistance and the LRS resistance of the device is close to $5\times10^{6}\,\Omega$ and $1\times10^{3}\,\Omega$.

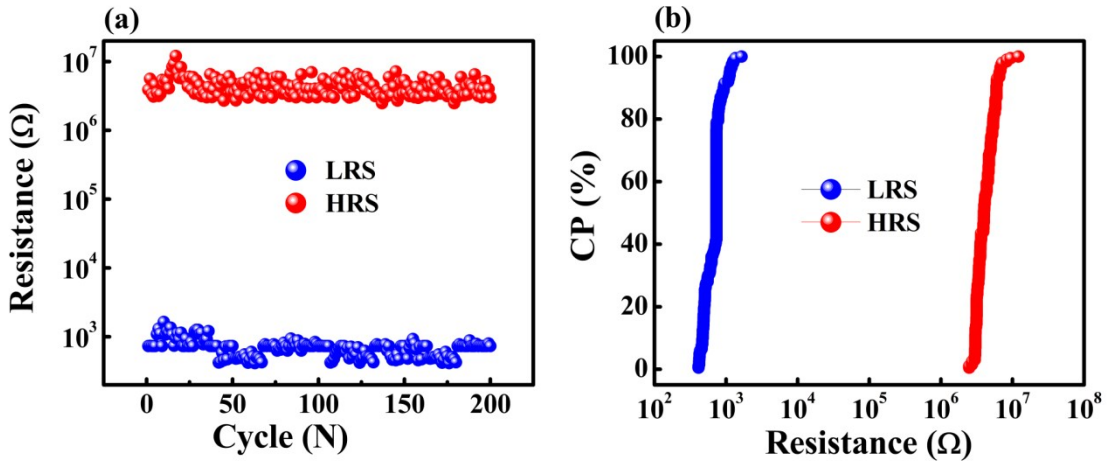

Figure S4. (a) Switch resistance of Ag/ZHO/GOQDs/ZHO/Pt device. (b) Statistic resistance distributions of the 200 I-V cycles sweeping. Cumulative probability is abbreviated as CP.

Ⅴ Endurance measurement of Ag/ZHO/GOQDs/ZHO/Pt device

The electrical pulse-induced resistive switching characteristic of the GOQDs device is shown in Fig. S5. The pulse of 2V/150ns and -2V/150ns were defined as programming and erasing voltage pulse, and 0.1V/1000ns voltage pulse was applied to read the resistance of the device as shown in Fig. S5(a). It should be noted that a stable resistive switching is observed up to 1×10^6 cycles as shown in Fig. S5(b). After 1×10^6 successive switching cycles, the resistance ratios between HRS and LRS are still has no apparent degradation. It indicates that the GOQDs memory device possesses overwhelming endurance property.

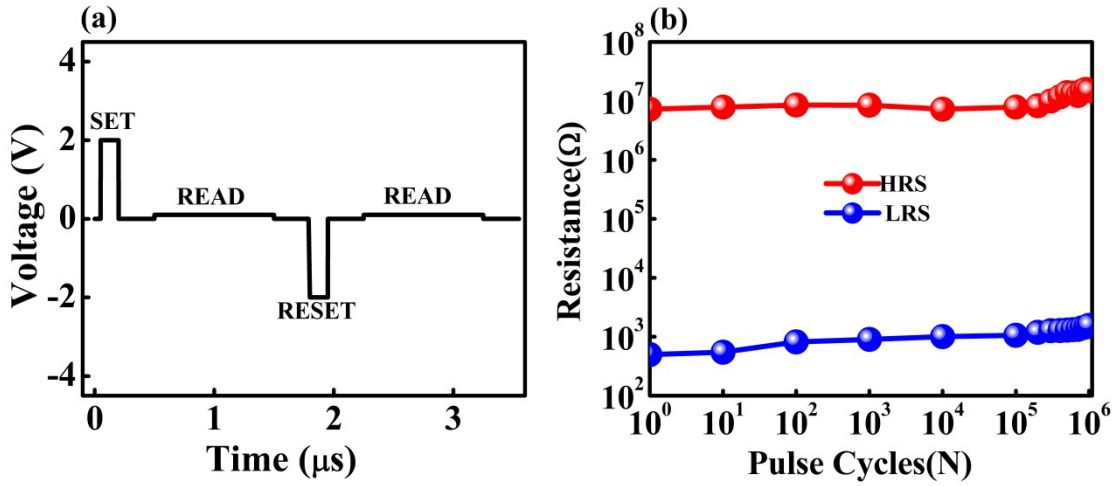

Figure S5. Endurance test of Ag/ZHO/GOQDs/ZHO/Pt device under pulse mode. (a) Pulses with 2V/150ns and -2V/150ns for set and reset, 0.1V/1000ns for reading. (b) Endurance property for 10^6 pulse cycle.

Ⅵ The double-logarithmic I-V curve of the GOQDs device

To clarify the conduction mechanisms of oxide-based devices with embedded GOQDs, the positive and negative sweep region about I-V curves of the device with GOQDs in double-logarithmic scale are depicted in Figs. S6(a) and S6(b). Usually the typical I-V characteristics of the trap-controlled space charge limited current (SCLC) consists of three parts: linear relationship between I-V (ohmic contact), the current proportional to the square of the voltage ($I\text{-}V^2$), and the dramatically increased I with the increase of V.[4, 5] We can see that at the positive sweep region, the I-V curves in HRS display ohmic behavior with the slope1 is 0.98, Child's law with the square relation when the slope2 is 1.88, and a steep current rise when the slpoe3 is 3.86 and very large slope at set region. In a word, the fitting results for HRS explain that the charge transport behavior during set process is in good agreement with the classical SCLC mode. At the negative sweep region, the I-V characteristics in HRS also basically follow the trap-controlled SCLC mechanism. In both the LRS at the positive and negative region, both the fitted slopes are close to 1, which indicate that they are ohmic conduction behavior. So it suggests the formation of conductive filaments during the set process.

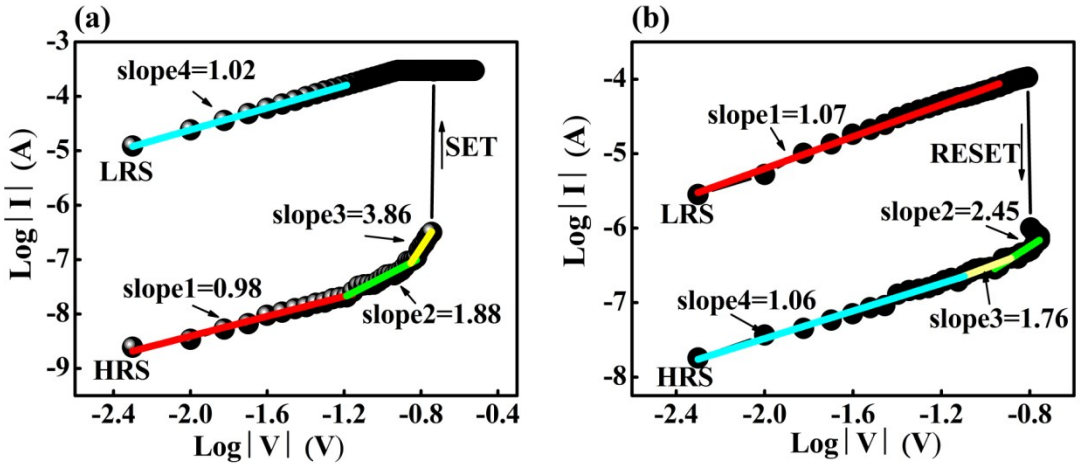

Figure S6. Piecewise linear fitting for the double-logarithmic I-V curve of the GOQDs device. (a) Positive sweep region. (b) Negative sweep region.

Ⅶ Comparison on switching voltage and OFF/ON ratio

Device structure	OFF/ON ratio	V_S/V_R	References
Ti/CdSe QDs/Ti-TiO_2/CdSe QDs/ITO	~10^2	-1V/1.5-2V	6
Al/CdSe QDs/Al/CdSe QDs/ITO	~10^4	-0.45V/2V	7
Al/[PMMA:CdSe /ZnS QD]/PMMA/[PMMA:CdSe /ZnS QD]/ITO	~10^4	-1.2V/3V	8
Al/In_2O_3/CdSe QD /ITO	~10^3	-1V/2V	9
Ag/(Graphene QDs/PVP)/Ag	~14	1.5V/-1.65V	10
Au/PMMA/PMMA:MoS_2 QDs/PMMA/FTO	~10^2	0.5V/-0.9V	11
Ag/ZHO/GOQDs/ZHO/Pt	~10^4	0.08-0.3V/-0.14--0.01V	This work

Table S1. Comparison of switching parameters with literatures. From the table , we can see that the RRAM with GOQDs we prepared has a smaller V_S and V_R.

References

1 D. Liu, H. Cheng, X. Zhu, G. Wang and N. Wang, *ACS Appl. Mat. Interfaces*, 2013,**5**,11258.

2 Y. Sharma, P. Misra, S. P. Pavunny and R. S. Katiyar, *Appl. Phys. Lett.*, 2014, **104**, 073501.

3 R. Zhang, J. Miao, F. Shao, W.T. Huang, C. Dong, X.G. Xu and Y. Jiang, *J. Non-Cryst. Solids*, 2014, **406**, 102-106.

4 Q. Liu, W. Guan, S. Long, R. Jia and M. Liu, J. Chen, *Appl. Phys. Lett.*, 2008, **92**, 012117.

5 L. G. Wang, Z. Y. Cao, X. Qian, L. Zhu, D. P. Cui, A. D. Li and D. Wu, *ACS Appl. Mater. Interfaces*, 2017, **9**, 6634-6643.

6 V. Kannan and J. K. Rhee, *J. Appl. Phys*., 2011, **110**, 074505.

7 V. Kannan and J. K. Rhee, *Appl. Phys. Lett*., 2011, **99**, 143504.

8 Z. H. Ma, C. X. Wu, D. U. Lee, F. S. Li and T. W. Kim, *Org. Electron*., 2016, **28**, 20-24.

9 S. Ali, J. Bae, C. H. Lee, K. H. Choi and Y. H. Doh, *Org. Electron*., 2015, **25**, 225-231.

10 I. V. Antonova, N. A. Nebogatikova and V. Y. Prinz, *J. Appl. Phys*., 2016, **119**, 224302.

11 D. L. Wang, F. Z. Ji, X. M. Chen, Y. Li, B. F. Ding and Y. Zhang, *Appl. Phys. Lett*., 2017, **110**, 093501.